Defense Technical Information Center Compilation Part Notice

ADP020040

TITLE: Laser Induced Retinal Damage Thresholds for Annular Retinal Beam Profiles

DISTRIBUTION: Approved for public release, distribution unlimited

This paper is part of the following report:

TITLE: Laser Interaction with Tissue and Cells XV. Held in San Jose, Ca on 26-28 January 2004.

To order the complete compilation report, use: ADA436676

The following component part numbers comprise the compilation report:
ADP020007 thru ADP020056

Laser induced retinal damage thresholds for annular retinal beam profiles

Paul K. Kennedy[a], Joseph A. Zuclich[b], David J. Lund[c], Peter R. Edsall[b], Stephen Till[d], Bruce E. Stuck[c], and Richard C. Hollins[d]

[a]US Air Force Research Lab, 2650 Louis Bauer Dr., Brooks City-Base, TX, USA 78235;
[b]Northrop-Grumman IT, 4241 Woodcock Dr., Suite B-100, San Antonio, TX, USA 78228;
[c]US Army Medical Research Det., 7965 Dave Irwin Dr., Brooks City-Base, TX, USA 78235;
[d]UK Defense Science & Technology Laboratory, Malvern, Worcs WR143PS, UK.

ABSTRACT

The dependence of retinal damage thresholds on laser spot size, for annular retinal beam profiles, was measured *in vivo* for 3 μs, 590 nm pulses from a flashlamp-pumped dye laser. Minimum Visible Lesion (MVL) ED_{50} thresholds in rhesus were measured for annular retinal beam profiles covering 5, 10, and 20 mrad of visual field; which correspond to outer beam diameters of roughly 70, 160, and 300 μm, respectively, on the primate retina. Annular beam profiles at the retinal plane were achieved using a telescopic imaging system, with the focal properties of the eye represented as an equivalent thin lens, and all annular beam profiles had a 37 % central obscuration. As a check on experimental data, theoretical MVL-ED_{50} thresholds for annular beam exposures were calculated using the Thompson-Gerstman granular model of laser-induced thermal damage to the retina. Threshold calculations were performed for the three experimental beam diameters and for an intermediate case with an outer beam diameter of 230 μm. Results indicate that the threshold vs. spot size trends, for annular beams, are similar to the trends for top hat beams determined in a previous study; i.e., the threshold dose varies with the retinal image area for larger image sizes. The model correctly predicts the threshold vs. spot size trends seen in the biological data, for both annular and top hat retinal beam profiles.

Keywords: laser, eye, retina, image profile, spot size, annular beam, lesion, damage threshold, thermal model.

1. INTRODUCTION

Over the past three decades, the U.S. Department of Defense has funded world-class research in the areas of laser safety, laser eye protection, and laser bioeffects, with the goal of protecting pilots and other military personnel from laser-induced eye damage. Retinal injuries produced by ocular exposure to visible and near-infrared laser pulses have been of particular concern.[1-3] For ultrashort pulses, the damage produced at the retina may be increased by nonlinear optical processes in the eye, such as self-focusing and laser-induced breakdown.[4] These processes, however, also offer the potential for broadband laser eye protection, using nonlinear optical limiters.[5-9]

Nonlinear optical limiter cells have been constructed using a wide variety of materials, including organics, fullerenes, semiconductors, and carbon-black suspensions.[5,6] They provide ocular protection through linear and nonlinear absorption, which reduce the transmitted laser energy, and through nonlinear scattering and refraction, which increase the retinal image size and distribute the transmitted energy across a larger retinal area.[7-9] The latter effect, which essentially causes the output of the limiter cell to be an extended source, complicates assessment of the biological effects of limiters and of the degree of optical protection provided. Current national and international laser safety standards[10,11] provide guidance on maximum permissible exposures for extended sources; however, these standards are based on a limited amount of biological data. Few studies available in the literature give biological measurements of the variation in retinal damage threshold as a function of input beam divergence or retinal image size. Many of the older studies give only a small number of data points.[12,13]

Laser Interaction with Tissue and Cells XV, edited by Steven L. Jacques, William P. Roach, Proc. of SPIE Vol. 5319 (SPIE, Bellingham, WA, 2004) · 1605-7422/04/$15 · doi: 10.1117/12.529400

Over the past ten years, the U.K. Ministry of Defense and the U.S. Department of Defense have funded international collaborative studies on the biological effects of nonlinear optical limiters[9] and on the variation in retinal damage thresholds as a function of retinal image size.[14-17] The damage studies were done using nanosecond and microsecond duration laser pulses at visible wavelengths, with Gaussian (small beam) or top hat (large beam) retinal image profiles. The biological studies were supplemented by theoretical calculations using the Thompson-Gerstman granular model of laser-induced thermal damage to the retina.[18-20]

The study documented in this paper is a continuation of our earlier work, now extended to include annular, as well as top hat, retinal beam profiles. The dependence of retinal damage thresholds on laser spot size, for annular retinal beam profiles, was measured *in vivo* and calculated theoretically, for beam profiles covering up to 20 mrad of visual field on the primate retina. Both experimental and theoretical results indicate that the threshold vs. spot size trends, for annular beams, are similar to the trends for top hat beams determined previously; i.e., the threshold dose varies with the retinal image area for larger image sizes.

2. EXPERIMENTAL THRESHOLD STUDY

The subjects used in the experimental threshold study were rhesus monkeys (*Macaca mulatta*). All animals involved were procured, maintained, and used in accordance with the Animal Welfare Act and the "Guide for the Care and Use of Laboratory Animals" prepared by the Institute of Laboratory Animal Resources, National Research Council; and the ARVO Resolution on the Use of Animals in Research. Appropriate levels of anesthesia were used in all experiments, so the subjects did not experience pain or distress. Pre-exposure screening of subjects, to insure clear ocular media and normal retinas, consisted of slit-lamp and fundus camera examinations, fluorescein angiography, and refraction to the nearest 0.25 diopter.

Minimum Visible Lesion (MVL) ED_{50} retinal damage thresholds in rhesus were measured *in vivo* using the experimental set-up shown in Figure 1. A flashlamp-pumped dye laser, taken from a clinical photocoagulation instrument (Candela Model LFDL-8), was used to obtain 590 nm emission (rhodamine 6G dye), with a maximum pulse energy of 1 J and a 3 μs pulsewidth. An external trigger switch was used to trigger single pulses for delivery to each retinal exposure site. The beam diameter at the laser output was ~ 6 mm, with poor transverse mode quality. As shown in Figure 1, a beam expander and an annular aperture were used to yield a clean, collimated annular beam, with an outer diameter of 15.9 mm, an inner (obscuration) diameter of 9.8 mm, and a 38 % annular obscuration ratio. This beam served as the source annulus for creation of the three annular retinal beam profiles used in the threshold study.

Annular beam profiles at the retinal plane were achieved using a telescopic imaging system, with the focal properties of the eye represented as an equivalent thin lens. The elements of the imaging system, shown in Figure 1, were a focusing lens of variable power, a turning flat, and the rhesus eye. Annular retinal beam profiles were created covering approximately 5, 10, and 20 mrad of visual field; which correspond to outer beam diameters of roughly 70, 160, and 300 μm, respectively, on the primate retina. The annular obscuration ratios were 37 % for the two larger beams and 33 % for the 5 mrad beam. Retinal irradiance profiles for the three annular beams are shown in Figure 2 and the exact experimental parameters for all annular beams used in the study are given in Table 1.

When the subject was absent, the reflected laser was directed into a detector, which measured the total pulse energy that would have entered the dilated pupil of the subject's eye. Pulse energy was measured by two Laser Precision RJP 735 detectors coupled to a Laser Precision RJ 7620 energy ratiometer. Other experimental details, including alignment of the beam with the retinal target site using a fundus camera, positioning of the subject, and placement of marker lesions, were identical to procedures described in detail in earlier studies[16,17] and will be omitted for brevity.

Lesion/ no lesion readings were conducted for each exposed eye via ophthalmoscopic observation at 1-hour and 24-hours post exposure. The binary lesion/no lesion data were used to calculate the MVL-ED_{50} thresholds, and 95 % confidence intervals (fiducial limits), by probit analysis. Observation of the exposed sites indicated that annular beams covering 5 mrad of visual field on the retina (~ 70 μm in diameter) create solid retinal lesions, that differ little in appearance and threshold energy from those created by top hat beams of equal size. Annular beams of 10 and 20 mrad, however, create annular retinal lesions of a size (~ 160 and 300 μm in diameter, respectively) equal to the retinal image size. An example

is given in Figure 3, a fundus photograph showing 20 mrad annular lesions at one hour post exposure. A white circle representing the expected energy distribution at the retina is also shown for comparison.

In Table 2, we list the experimental MVL-ED_{50} retinal damage thresholds as a function of retinal image size for both Top Hat (Disc) and Annular retinal beam profiles. The top hat data, for 5 and 20 mrad beams, was taken from our earlier work[16,17] and is included for comparison. Thresholds are given as total intraocular energy (dose) for exposures in both the macular and paramacular regions, and at 1-hour and 24-hours post exposure. The macular and paramacular threshold energies from Table 2 are plotted as a function of retinal image diameter in Figures 4 and 5, respectively. Threshold data for 1.5 mrad (~ 22 μm diameter) top hat beams, again taken from our earlier work,[16,17] have also been included in Figures 4 and 5 for comparison.

3. THEORETICAL THRESHOLD STUDY

As a cross check on experimental results, theoretical retinal damage thresholds were calculated for equivalent (3 μs, 590 nm) pulsed exposures, using the Thompson-Gerstman granular model of laser-induced thermal damage to the retina. Theoretical MVL-ED_{50} thresholds were calculated for annular retinal beam profiles with outer beam diameters of 70, 160, 230, and 300 μm, and a 37 % central obscuration. For purposes of comparison, theoretical thresholds were also calculated for top hat retinal beam profiles, with the same four retinal beam diameters. The outer diameter of the incident laser beam was assumed to fill a 7 mm pupil at the cornea and optical transmission to the retina was assumed, for simplicity, to be 100%. The biological input parameters used in these runs (i.e., the melanosome values for rhesus retinal pigmented epithelium) were the same as those used in previous studies:[16,17] melanosome radius – 1 μm; thickness of the retinal pigmented epithelium (RPE) layer – 15 μm; volume of an RPE cell – 6×10^{-9} cm^3; melanosomes per RPE cell – 50; and melanosome absorption coefficient – 4,000 cm^{-1}.

For top hat beams, the damage integral was evaluated in the center of the beam, with a damage spot 20 μm in diameter used as the calculational endpoint representing an MVL. For annular beams, the damage integral was evaluated at the midpoint of the annulus, with an annular damage spot, whose diameter was equal to the diameter of the annular beam, used as the calculational endpoint. The resulting theoretical damage thresholds are listed in Table 3. The thresholds are given in terms of intraocular energy (for comparison to the experimental values of Table 2), as well as in terms of fluence (energy/unit area) at the cornea and retina.

4. DISCUSSION OF RESULTS

Comparison of Tables 2 and 3 shows that the energy thresholds calculated by the model are consistently higher than experimentally measured values. We believe this is largely due to the fact that biologically accurate input parameters, for melanosome size, spatial distribution, number density (granules/cell) and absorption coefficient, are not currently known. A histopathology research program is now in progress, which should produce accurate measurements of these melanosome parameters for rhesus RPE. In the interim, however, the model does seem to accurately predict the threshold versus spot size trends, for both top hat and annular beams. This makes it a useful cross check for the experimental results in this study.

The 5 mrad threshold energies from Table 2 differ little for top hat and annular beams. In contrast, the 24-hour macular energy threshold for a 20 mrad annular beam is lower (~ 83 %) than the equivalent threshold for a 20 mrad top hat beam. This agrees well with the Annular/Top Hat energy ratios for the theoretical retinal thresholds shown in Table 3 (85-88 %). Although the energy threshold is lower for annular beams, Table 3 shows that the annular retinal fluence threshold is higher, due to the 37 % annular obscuration. The lower annular threshold energy, distributed over the smaller annular beam area, gives an Annular/Top Hat retinal fluence ratio of 1.4 (0.88/0.63). The equivalent experimental value for the 20 mrad, 24-hour macular thresholds is 1.32 (0.83/0.63).

The equivalence of the 5 mrad threshold energies, for top hat and annular exposures, is consistent with the ophthalmic observation, mentioned in Section 2, that 5 mrad annular beams create solid retinal lesions similar in appearance to those created by 5 mrad top hat beams. It would appear that a solid lesion is created, for smaller beams, because flow of heat from the outer beam edges does not significantly reduce flow of heat into the annular obscuration area. On the other

hand, 10 and 20 mrad annular beams create annular retinal lesions because there is insufficient inward heat flow, at threshold fluences, to create tissue damage in the obscuration region. This double heat flow, both inward and outward from the annular region exposed, also explains why higher retinal fluences (1.4/1.0) are required to create annular, as opposed to solid, retinal lesions.

From Table 3, we see that the theoretical thresholds, for both annular and top hat beams, showed the same trends with spot size; i.e., retinal fluence thresholds were essentially constant for retinal beam profiles with outer beam diameters greater than 160 μm. Similar trends in theoretical damage thresholds were seen in previous studies,[16,17] for much larger top hat beams (up to 1400 μm in diameter). There the threshold dose varied with the retinal image area (i.e., constant retinal fluence) for beam diameters greater than (roughly) 140 μm.

As we see from Figures 4 and 5, trends in the biological data are somewhat more ambiguous than those predicted by the model. The slope of the threshold energy plots does not quite reach a value of two (constant retinal fluence), possibly because the study only used beam diameters of 300 μm or less. In the previous top hat beam study,[16,17] exposures were done for beams of up to 1600 μm in diameter, producing a much clearer trend towards constant retinal fluence thresholds. The inflection point in the biological data (beam diameter corresponding to constant fluence threshold) was also clearer for the previous (larger beam) data; it occurred at beam diameters of roughly 100-150 μm. In Figures 4 and 5, the lack of data for beams larger than 300 μm seems to suggest an inflection point at much smaller beam diameters; however, we believe this is an artifact of the smaller data set. Taking these factors into consideration, we believe that the model predicts the threshold vs. spot size trends seen in the biological data with reasonable accuracy, for both annular and top hat retinal exposures.

5. CONCLUSIONS

The dependence of retinal damage thresholds on laser spot size, for annular retinal beam profiles, was measured *in vivo* for 3 μs, 590 nm laser pulses. MVL-ED_{50} thresholds in rhesus were measured for annular retinal beam profiles covering 5, 10, and 20 mrad of visual field; which correspond to outer beam diameters of roughly 70, 160, and 300 μm, respectively, on the retina. As a cross check on experimental results, theoretical retinal damage thresholds were calculated for equivalent pulsed exposures, using the Thompson-Gerstman model. Theoretical thresholds were calculated for annular retinal beam profiles with outer beam diameters of 70, 160, 230, and 300 μm, and a 37 % central obscuration. For purposes of comparison, theoretical thresholds were also calculated for top hat retinal beam profiles, with the same beam diameters. Results indicate that the threshold vs. spot size trends, for annular beams, are similar to the trends for top hat beams; i.e., the threshold dose varies with the retinal image area for larger image sizes. The model correctly predicts the threshold vs. spot size trends seen in the biological data, for both annular and top hat retinal beam profiles.

ACKNOWLEDGMENTS

This work was supported by: i) the Optical Radiation Branch of the US Air Force Research Laboratory; ii) Northrop-Grumman Information Technologies; iii) the US Army Medical Research Detachment; iv) the Air Force Office of Scientific Research, under the International Research Initiatives (IRI) program, LRIR # 01HE13THE; and v) the UK Defence Science & Technology Laboratory (UK/DSTL), through Contract # RD018-07411 .

REFERENCES

1. R. Birngruber, C. A. Puliafito, A. Gawande, W.-Z. Lin, R. W. Schoenlein, and J. G. Fujimoto, "Femtosecond laser-tissue interactions: retinal injury studies," IEEE J. Quantum Electron., vol. QE-23, pp. 1836-1844, 1987.

2. J. A. Zuclich, W. R. Elliott, and D. J. Coffey, "Suprathreshold retinal lesions induced by laser radiation," Lasers Light Ophthalmol., vol. 5, pp. 51-59, 1992.

3. C. P. Cain, C. A. Toth, C. D. DiCarlo, C. D. Stein, G. D. Noojin, D. J. Stolarski, and W. P. Roach, "Visible retinal lesions from ultrashort laser pulses in the primate eye," Invest. Ophthalmol. Vis. Sci., vol. 36, pp. 879-888, 1995.

4. P. K. Kennedy, D. X. Hammer, and B. A. Rockwell, "Laser-induced breakdown in aqueous media," Prog. Quantum Electron., vol. 21, pp. 155-248, 1997.

5. L. W. Tutt and T. F. Boggess, "A review of optical limiting mechanisms and devices using organics, fullerenes, semiconductors and other materials," Prog. Quantum Electr., vol. 17, pp. 299-338, 1993.

6. K. Mansour, M. J. Soileau, and E. W. Van Stryland, "Nonlinear optical properties of carbon-black suspensions (ink)," J. Opt. Soc. Am. B, vol. 9, pp. 1100-1109, 1992.

7. E. W. Van Stryland, H. Vanherxeele, M. A. Woodall, M. J. Soileau, A. L. Smirl, S. Guha, and T. F. Boggess, "Two-photon absorption, nonlinear refraction, and optical limiting in semiconductors," Opt. Eng., vol. 24, pp. 613, 1985.

8. M. Shiek-Bahae, A. A. Said, D. J. Hagan, M. J. Soileau, and E. W. Van Stryland, "Nonlinear refraction and optical limiting in thick media," Opt. Eng., vol. 30, pp. 1228, 1991.

9. J. A. Zuclich, "Study of ocular protection provided by non-linear optical switches," Final Report, TASC, Contract ELM/0874 (UK Defense Research Agency, Malvern, U.K., 1996).

10. ANSI Standard Z136.1-2000: American National Standard for Safe Use of Lasers, (American National Standards Institute, New York, 2000).

11. IEC 60825-1-2001: Safety of Laser Products – Part 1: Equipment Classification, Requirements and User's Guide, (International Electrotechnical Commission, Geneva, Switzerland, 2001).

12. D. Sliney and M. Wolbarsht, Safety with Lasers and Other Optical Sources, (Plenum Press, New York, 1980).

13. D. Courant, L. A. Court, and D. H. Sliney, "Research relative to safety formulations for retinal damage from extended sources and large retinal images," Proc. Inter. Laser Safety Conf., Sect. 4, pp. 25-33, 1990.

14. J. A. Zuclich, D. J. Lund, P. R. Edsall, R. C. Hollins, P. A. Smith, B. E. Stuck, and L. N. McLin, "Laser induced retinal-damage as a function of retinal image size," Proc. SPIE, vol. 3591, pp. 335-343, 1999.

15. J. A. Zuclich, D. J. Lund, P. R. Edsall, R. C. Hollins, P. A. Smith, B. E. Stuck, and L. N. McLin, "Experimental study of the variation of laser-induced retinal damage threshold with retinal image size (microsecond pulsewidths)," Nonlinear Opt., vol. 21, pp. 19-28, 1999.

16. J. A. Zuclich, P. R. Edsall, D. J. Lund, B. E. Stuck, R. C. Hollins, S. Till, P. A. Smith, L. N. McLin, and P. K. Kennedy, "Variation of laser induced retinal-damage threshold with retinal image size," J. Laser Appl., vol. 12, pp. 74-80, 2000.

17. J. A. Zuclich, D. J. Lund, P. E. Edsall, S. Till, B. E. Stuck, R. C. Hollins, and P. K. Kennedy, "New data on the variation of laser induced retinal-damage threshold with retinal image size," Proceedings of the Laser Bioeffects Meeting, held in Paris, France, June 13-14, 2002.

18. C. R. Thompson, "Melanin granule model for heating of tissue by laser," Proc. SPIE, vol. 2134A, pp. 66-77, 1994.

19. C. R. Thompson, B. S. Gerstman, S. L. Jacques, and M. E. Rogers, "Melanin granule model for laser-induced thermal damage in the retina," Bull. Math. Biol., vol. 58, pp. 513-553, 1996.

20. P. K. Kennedy, J. J. Druessel, J. M. Cupello, S. Till, B. S. Gerstman, C. R. Thompson, and B. A. Rockwell, "Parameter sensitivity of the Thompson granular retinal damage model," Proc. SPIE, vol. 3254A, pp. 146-155, 1998.

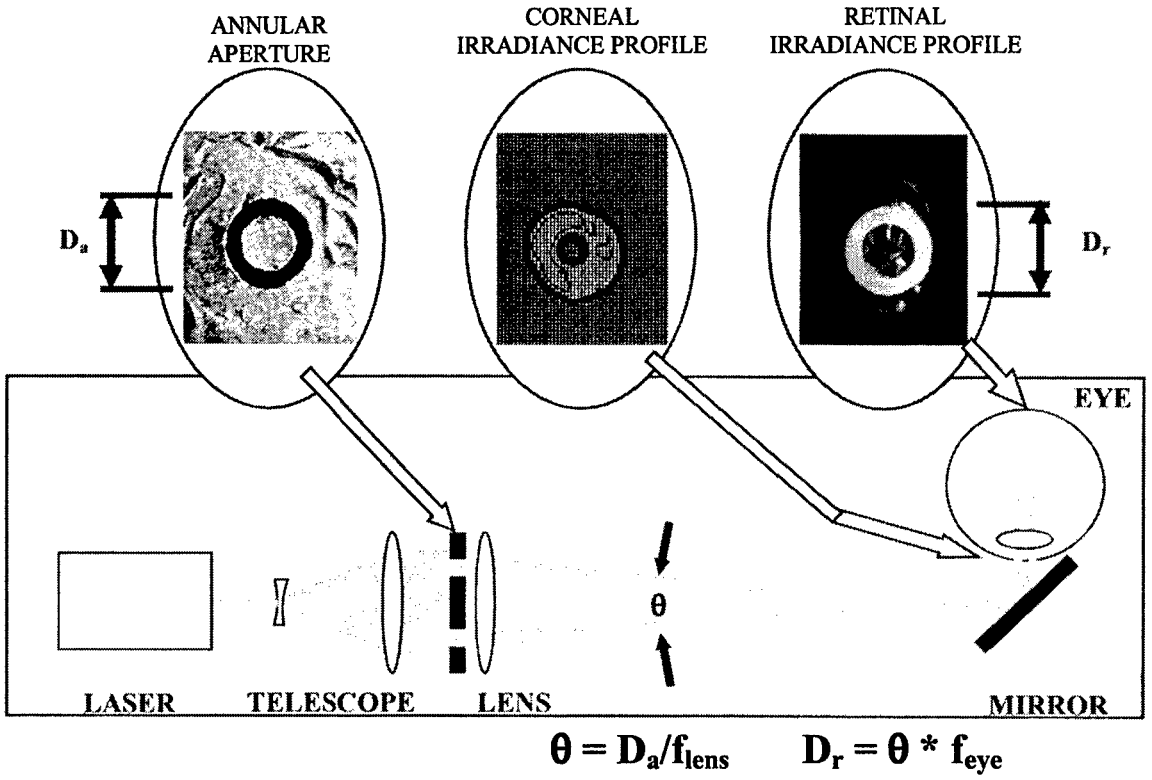

Figure 1 – Schematic diagram of experimental set-up.

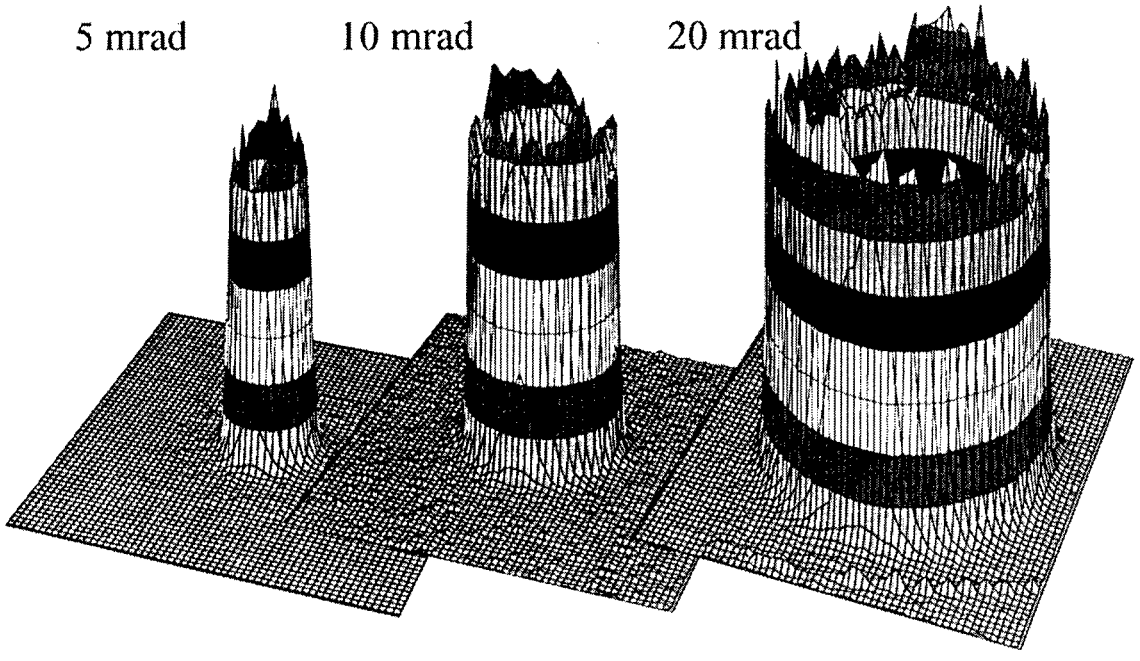

Figure 2 – Annular retinal image profiles for 5, 10, and 20 mrad beams.

SOURCE ANNULUS				
OUTER DIAMETER			**15.9 mm**	
OCCLUDED DIAMETER			**9.8 mm**	
OCCLUDED AREA/OUTER AREA			**0.38**	
FOCUSING LENS (diopters) –		**0.37**	**0.75**	**1.37**
DIVERGENCE (mrad) –	**outer**	**5.5**	**12.1**	**22.1**
	occluded	**3.2**	**7.4**	**13.5**
RETINAL DIAMETER (μm) –	**outer**	**74**	**163**	**298**
(f_{eye} = 13.5 mm)	**occluded**	**43**	**99**	**182**
OCCLUDED AREA/OUTER AREA –		**0.33**	**0.37**	**0.37**

Table 1 – Experimental parameters for annular beams.

Figure 3 - Retinal image showing 20 mrad annular burns at one hour post exposure. The white circle represents the expected energy distribution at the retina.

	Beam Divergence mrad	Retinal Diameter μm	ED_{50}, macula		ED_{50}, paramacula	
			1 hour	24 hour	1 hour	24 hour
			μJ	μJ	μJ	μJ
Annulus	5.5	74	12.4	11.1	22.3	20.8
Disc	5.7	77	12.6	11.8	20.2	16.9
Annulus	12.1	163	31.3	24.8	48.0	39.3
Annulus	22.1	298	50.4	50.4	93.0	80.7
Disc	21.5	290	72.2	60.7	133	87.8

Table 2 – Experimental MVL-ED_{50} retinal damage thresholds as a function of retinal spot size for Disc (Top Hat) and Annular retinal beam profiles.

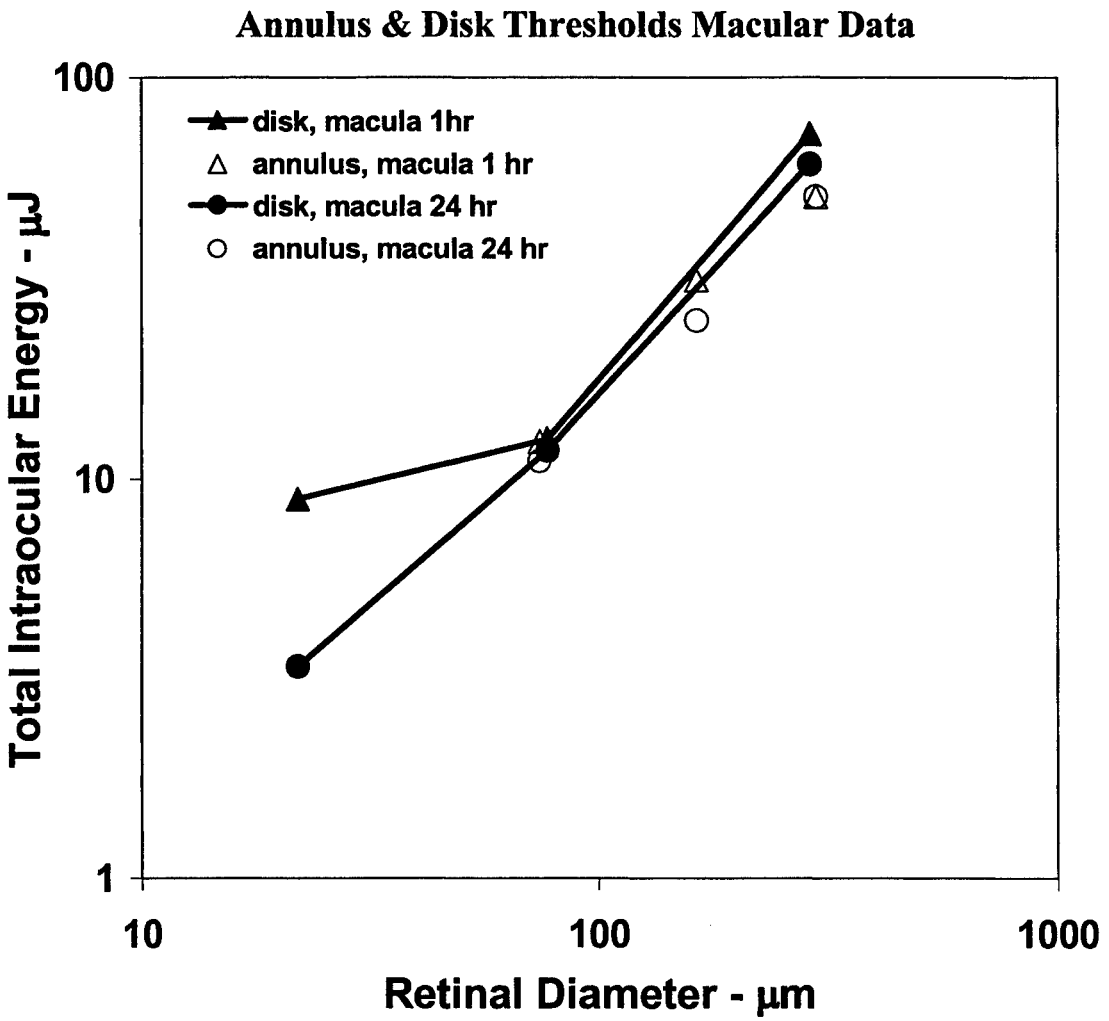

Figure 4 – Macular threshold data vs. retinal spot size.

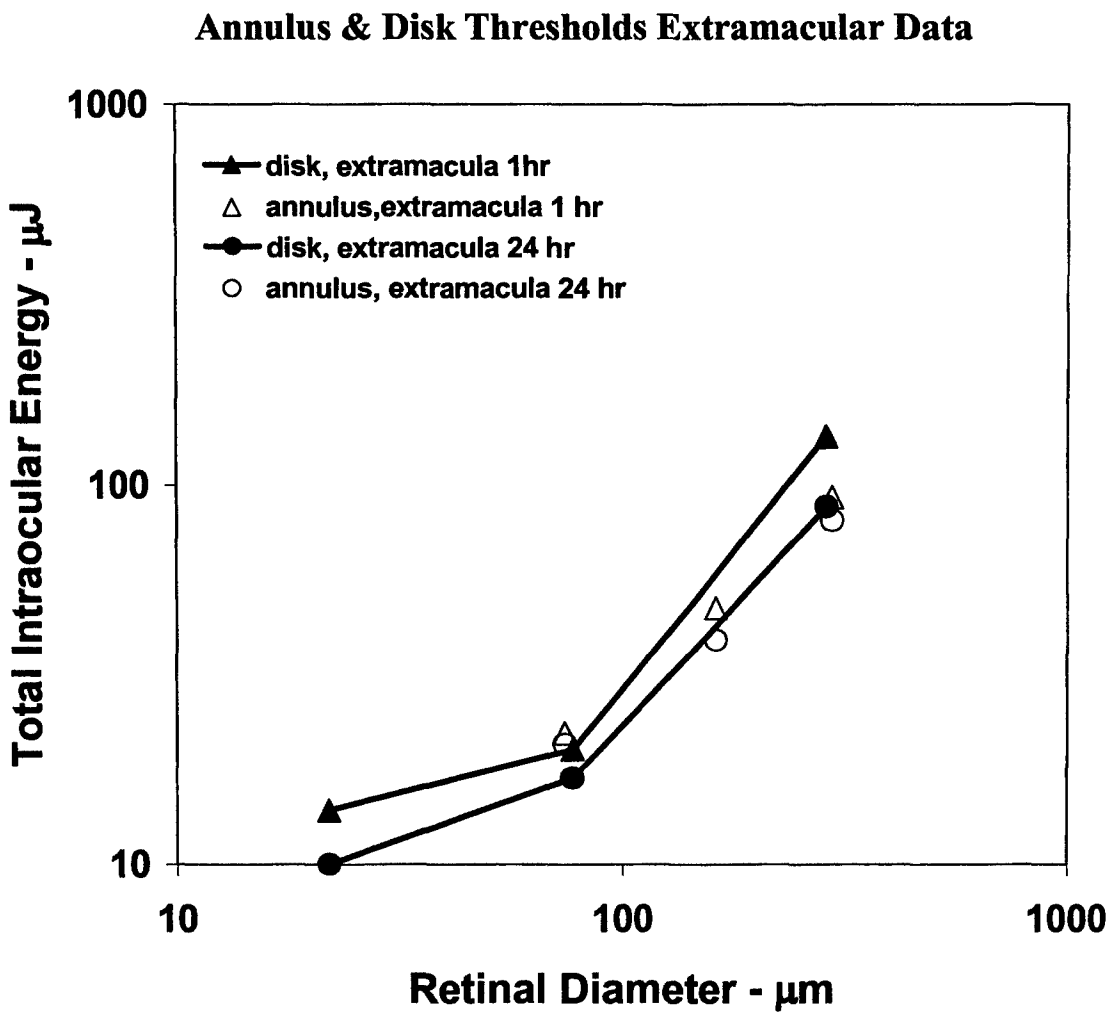

Figure 5 – Paramacular threshold data vs. retinal spot size.

τ_p, λ	d_r(µm)	E_{th}(µJ)	F_{th}(J/cm^2) --at Cornea	F_{th}(J/cm^2) --at Retina
$\tau_p = 3$ µs	300(TH)	918.92	2.4×10^{-3}	1.3×10^{0}
$\lambda = 590$ nm	230(TH)	540.12	1.4×10^{-3}	1.3×10^{0}
	160(TH)	261.38	6.8×10^{-4}	1.3×10^{0}
	70(TH)	57.73	1.5×10^{-4}	1.5×10^{0}
	300(AN)	800.09	3.3×10^{-3}	1.8×10^{0}
	230(AN)	460.66	1.9×10^{-3}	1.8×10^{0}
	160(AN)	230.33	9.5×10^{-4}	1.8×10^{0}
	70(AN)	50.92	2.1×10^{-4}	2.1×10^{0}

Table 3 – Theoretical MVL-ED_{50} retinal damage thresholds as a function of retinal spot size for Top Hat (TH) and Annular (AN) retinal beam profiles.